Scientia Iranica (2025) **32**(1): 6205

SCIENTIA IRANICA

Sharif University of Technology
Scientia Iranica
Transactions on Computer Science & Engineering and Electrical Engineering
https://scientiairanica.sharif.edu

Multi-port high-frequency AC-link and indirect matrix converters: A generalized structure

Hossein Hojabri*

Department of Electrical Engineering, Shahid Bahonar University of Kerman, Kerman 76169-14111, Iran.

Received 19 March 2022; received in revised form 07 May 2023; accepted 26 June 2023

KEYWORDS
AC/DC grid connection;
High-Frequency AC-link (HFAC) converter;
Indirect matrix converter;
Modulation method;
Multi-port converter.

Abstract. Conventional multi-stage AC/DC/DC, AC/DC/AC, DC/DC/DC, and DC/DC/AC converters are two ports converters used to connect a resource or load to an AC or DC grid. To connect several loads or resources to a grid, these converters can easily be extended to a multi-port converter through a common DC-link, with simplified control and a reduced number of active switches. However, DC-link huge energy storage component increases the converter volume and cost and reduces its lifetime and reliability. On the other hand, most of the resources with these types of converters have fault ride-through problems and the DC-link voltage increases during the grid-side faults. The indirect matrix converter is a two-port High-Frequency AC-link (HFAC) converter without any intermediate energy storage component, which can be used to connect just a single source or load to a grid. In this paper, a generalized extension of a two-port indirect matrix converter (and the other HFAC converters) to a multi-port converter is proposed. The modulation method, voltage and current gains, and the reactive power limitation of the proposed structure are also presented. Performances of the proposed structure and its modulation strategy are verified through simulation in MATLAB/SIMULINK environment.

1. Introduction

Distributed Generators (DGs) are connected to the AC or DC grids via conventional multi-stage AC/DC/AC, DC/DC/AC, AC/DC/DC, or DC/DC/DC converters, as presented in Figure 1(a). These converters are a back-to-back connection of two voltage source converters through a common DC-link capacitor. In a hybrid system with two or more DGs and storages, these converters can be easily extended to a multi-port converter with the back-to-back connection of multiple voltage source converter through their common DC-link capacitor, as shown in Figure 1(b) [1-5].

The intermediate DC-link capacitor simplifies the converter control through independent control of the DG-side and grid-side converters. The DG-side DC/DC or AC/DC converter controls the DG power and boosts its low voltage to a desirable level for the grid-side converter. The grid-side DC/AC or DC/DC converter controls the DC-link voltage by delivering generated power to the AC or DC grid. The DC/AC converter can also generate reactive power to meet the AC grid or load reactive power requirements [6].

Although the DC-link capacitor facilitates the converter control, it increases the converter volume, reduces its reliability, and causes grid-side fault ride-through problems [7]. When a fault occurs on the grid side, the grid-side converter voltage and power

*. *Corresponding author.*
E-mail address: hhojabri@uk.ac.ir (H. Hojabri)

To cite this article:
H. Hojabri "Multi-port high-frequency AC-Link and indirect matrix converters: A generalized structure", *Scientia Iranica* (2025), **32**(1): 6205 https://doi.org/10.24200/sci.2023.59375.6205

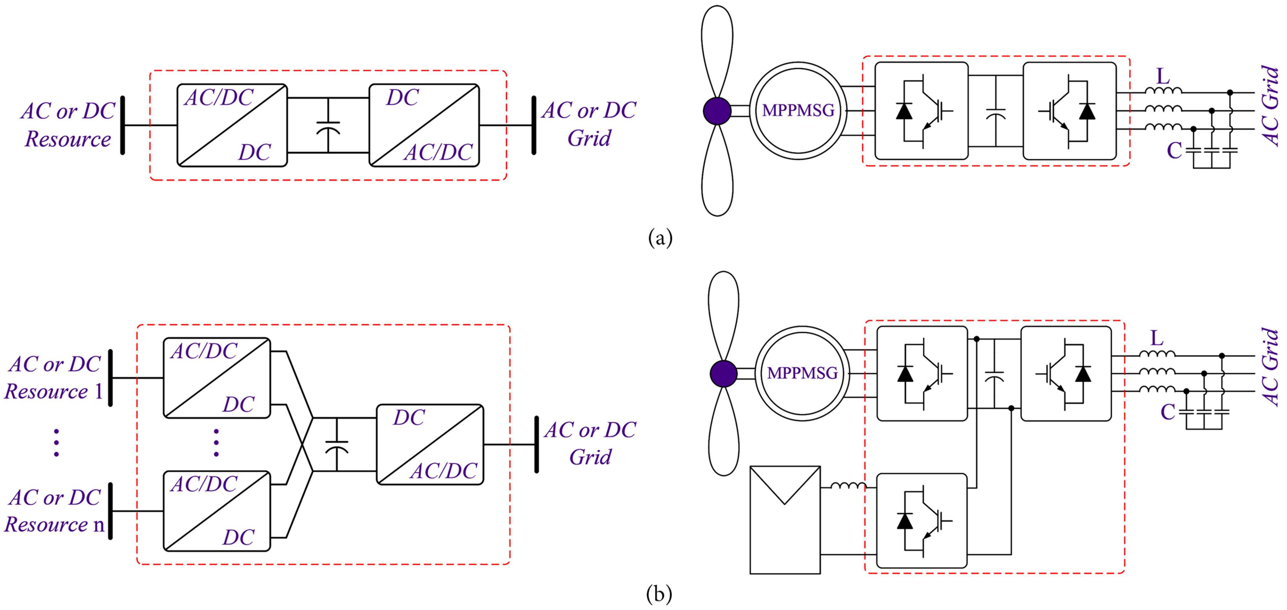

Figure 1. Structures of conventional back-to-back converters and an example of their application (a) Two-port converters and (b) Multi-port converters.

decrease, while the DG power cannot be decreased rapidly due to the independent control of the DG-side and grid-side converters. Therefore, the DC-link voltage increases due to its input and output power inequality. Two types of methods are proposed in the literature to solve this problem: adding an external system such as energy storage or a brake resistor, or improving the control structure of the DG-side converter by getting feedback from the DC-link or grid-side voltage. Both of these methods lead to the complexity of the converter structure or control [8-10]. For this purpose, direct and indirect matrix converters are proposed in the literature without any intermediate energy storage component. These all-silicon converters are more reliable and compact compared with the conventional multi-stage AC/DC/AC back-to-back frequency converters [11-13].

Due to the lack of an intermediate energy storage component, it is difficult to extend this two-port matrix converter to a multi-port one, and except for a few special and non-expandable three-port cases [14-22], most of the matrix converters proposed in the literature are two-port converters used to connect a single resource or load to an AC or DC grid. Therefore, to connect several resources or loads the grid, unlike extendable multi-stage back-to-back converters, several matrix converters are required which increases the system complexity and cost. In this paper, a generalized structure for multi-port indirect matrix converters is proposed which can be used to connect multiple DGs or storage to an AC or DC grid or load. The presented generalized structure can also be applied to the other High-Frequency AC-link (HFAC) converters.

For this purpose, in Section 2, the basic indirect matrix converter and its modulation method are investigated. The voltage and current gains of this converter are also presented in this section. In Section 3, the generalized structure of a multi-port indirect matrix converter is presented which can be used to connect multiple DC or AC DGs and storage to an AC or DC grid or load. Modulation and commutation methods of the proposed structure, and the voltage and current gains are also presented. Finally, the proposed generalized structure is verified through simulation in MATLAB/SIMULINK environment for different cases and conditions in Section 4 and conditions in Section 5.

2. Indirect matrix converter

The indirect matrix converter is a three-phase to three-phase HFAC converter without any intermediate energy storage component. The basic structure of a three-phase to three-phase indirect matrix converter is depicted in Figure 2. As presented in this figure, this converter is a back-to-back connection of two current source and voltage source converters with bidirectional four-quadrant switches. Although conventional indirect matrix converters are sparse counterparts of this basic topology with fewer active switches, in this manuscript just the basic topology is considered whose principles are applicable to all sparse topologies [23]. Due to the lack of huge energy storage components, these all-silicon converters are more compact and reliable compared with conventional back-to-back converters [24,25].

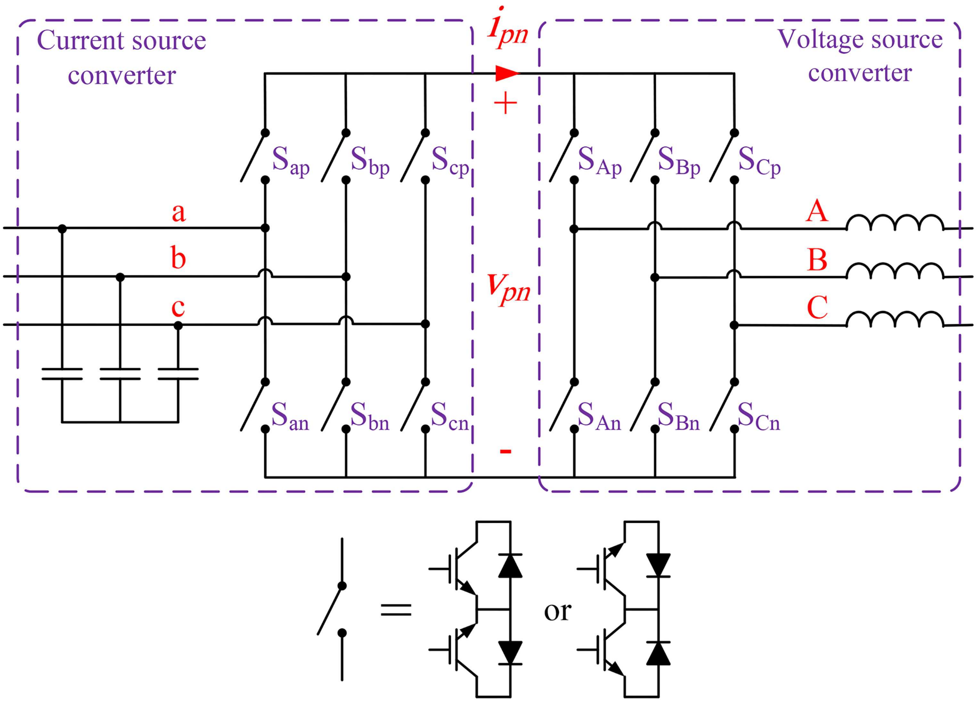

Figure 2. Schematic diagram of a three-phase to three-phase indirect matrix converter.

2.1. Modulation method

Since an indirect matrix converter is a back-to-back connection of a voltage source converter with a current source converter, one of the most complete modulation methods proposed for this converter is indirect Space Vector Modulation (SVM) [25,26]. In this modulation method, at first, it is supposed that the voltage source and current source converters of the indirect matrix converter are controlled independently by their conventional SVM methods and their switching states and times are calculated. Finally, calculated switching times and states are combined in the indirect SVM to control the indirect matrix converter the same as the back-to-back connection of a voltage source converter and a current source converter.

2.1.1. SVM of the voltage source converter

The voltage source converter of an indirect matrix converter is specified in Figure 2 which its voltage source value is v_{pn}. To control this voltage source converter, conventional SVM is used which its switching states and vectors are presented in Table 1 and Figure 3(a). Two of these vectors (i.e., $\vec{V}_7$ and $\vec{V}_8$) are zero vectors and the other remaining 6 vectors split $\alpha\beta$ plane into 6 sectors.

The desired output voltage vector $\vec{V}_{o,ref}$ in each sector of j can be constructed by the two adjacent vectors of this sector as presented in Figure 3(b). Hence, as depicted in Figure 3(c), for Dv_j portion of each switching period T_s vector $\vec{V}_j$, for Dv_{j+1} portion of T_s vector $\vec{V}_{j+1}$ and for the rest of the switching period vector $\vec{V}_0$ are applied. Dv_j, Dv_{j+1}, and Dv_0 can be obtained as follows:

$$\begin{cases} Dv_j = m_v \sin\left(\frac{\pi}{3} - \theta_v\right) \\ Dv_{j+1} = m_v \sin\left(\theta_v\right) \\ Dv_0 = 1 - Dv_j - Dv_{j+1} \end{cases} \tag{1}$$

where, m_v is the voltage source converter modulation index which controls the converter voltage gain as follows:

$$m_v = \sqrt{3}\frac{V_{o,ref}}{v_{pn,ave}}. \tag{2}$$

Table 1. The voltage source converter switching states and space vectors.

Vector name		Switching state	
$\mathbf{V_1}$	S_{Ap}	S_{Bn}	S_{Cn}
$\mathbf{V_2}$	S_{Ap}	S_{Bp}	S_{Cn}
$\mathbf{V_3}$	S_{An}	S_{Bp}	S_{Cn}
$\mathbf{V_4}$	S_{An}	S_{Bp}	S_{Cp}
$\mathbf{V_5}$	S_{An}	S_{Bn}	S_{Cp}
$\mathbf{V_6}$	S_{Ap}	S_{Bn}	S_{Cp}
$\mathbf{V_0}$ $\mathbf{V_7}$	S_{An}	S_{Bn}	S_{Cn}
$\mathbf{V_0}$ $\mathbf{V_8}$	S_{Ap}	S_{Bp}	S_{Cp}

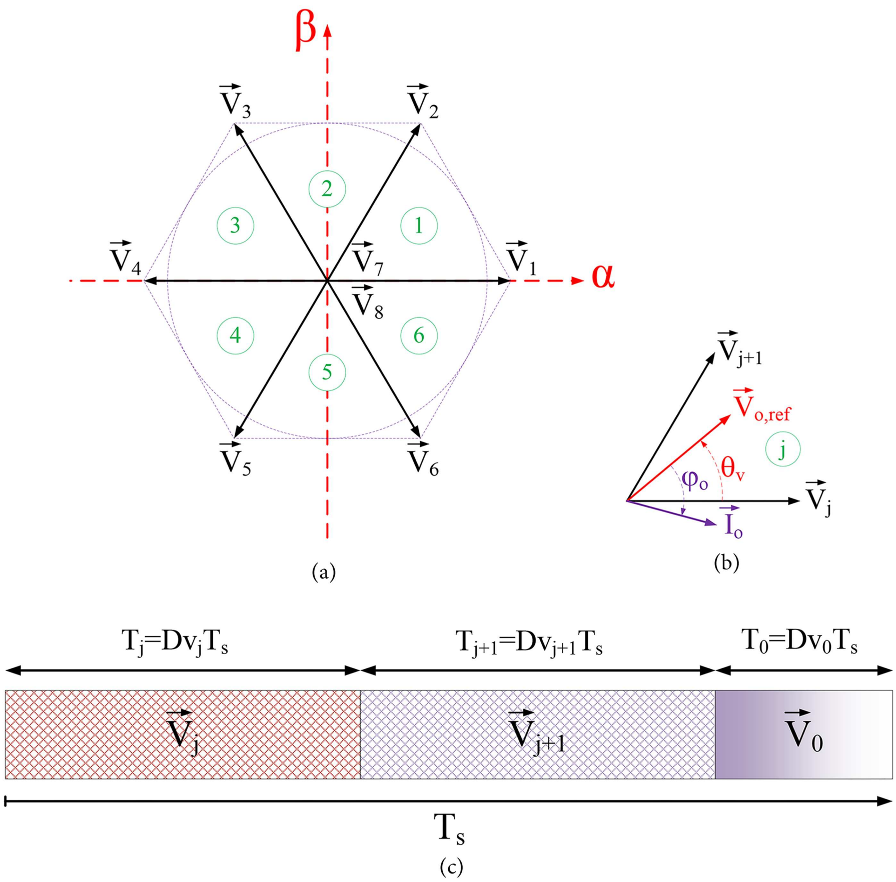

Figure 3. The voltage source converter space vectors in the $\alpha\beta$ reference frame and its SVM pattern.

$V_{o,ref}$ is the desired output phase to neutral voltage amplitude, and $v_{pn,ave}$ is the DC-link averaged voltage. The modulation index can be selected as $0 \leq m_v \leq 1$, and the maximum phase to neutral voltage amplitude which can be constructed with this modulation method is $\frac{v_{pn.ave}}{\sqrt{3}}$. The averaged output voltage and DC-link current of this voltage source converter is as follows:

$$\vec{V}_{o,ave} = Dv_j\vec{V}_j + Dv_{j+1}\vec{V}_{j+1} + Dv_0\vec{V}_0 = \vec{V}_{o,ref}, \quad (3)$$

$$i_{pn,ave} = \frac{3}{2v_{pn}}\{Dv_j\vec{V}_j.\vec{I}_o + Dv_{j+1}\vec{V}_{j+1}.\vec{I}_o\}$$

$$= \frac{\sqrt{3}}{2}m_vI_o\cos\varphi_o, \quad (4)$$

where, I_o and φ_o are the instantaneous output current amplitude and phase angle with respect to the output voltage.

2.1.2. SVM of the current source converter

The current source converter of an indirect matrix converter is specified in Figure 2 which its current source value is i_{pn}. To control this current source converter, conventional SVM is used which its switching vectors are presented in Table 2 and Figure 4(a). Three of these vectors (i.e., $\vec{I}_7$, $\vec{I}_8$, and $\vec{I}_9$) are zero vectors and the other remaining 6 vectors split $\alpha\beta$ plane into 6 sectors.

The desired input current vector $\vec{I}_{i,ref}$ in each sector of ⓚ can be constructed by the two adjacent vectors of this sector as presented in Figsure 4(b). Hence, as depicted in Figure 4(c), for Di_k portion of each switching period T_s vector $\vec{I}_k$, for Di_{k+1} portion of T_s vector $\vec{I}_{k+1}$, and for the rest of the switching

Table 2. The current source converter switching states and space vectors

Vector name		Switching state	
I₁		S_{ap}	S_{cn}
I₂		S_{bp}	S_{cn}
I₃		S_{bp}	S_{an}
I₄		S_{cp}	S_{an}
I₅		S_{cp}	S_{bn}
I₆		S_{ap}	S_{bn}
$\mathbf{I_0}$	$\mathbf{I_7}$	S_{ap}	S_{an}
	$\mathbf{I_8}$	S_{bp}	S_{bn}
	$\mathbf{I_9}$	S_{cp}	S_{cn}

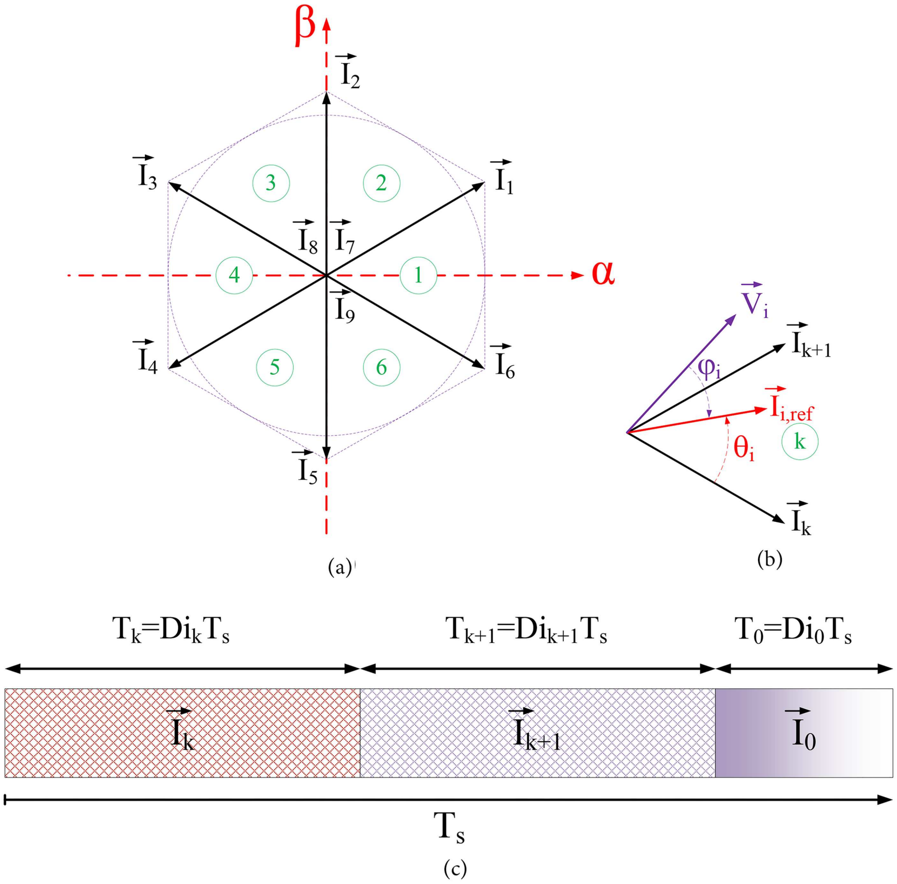

Figure 4. The current source converter space vectors in the $\alpha\beta$ reference frame and its SVM pattern.

period vector $\vec{I}_0$ are applied. Di_k, Di_{k+1}, and Di_0 can be calculated as follows:

$$\begin{cases} Di_k = m_c \sin\left(\frac{\pi}{3} - \theta_i\right) \\ Di_{k+1} = m_c \sin(\theta_i) \\ Di_0 = 1 - Di_k - Di_{k+1} \end{cases} \tag{5}$$

where, m_c is the current source converter modulation index which controls the converter current gain as follows:

$$m_c = \frac{I_{i,ref}}{i_{pn,ave}}, \tag{6}$$

$I_{i,ref}$ is the desired input current amplitude, and $i_{pn,ave}$ is the DC-link averaged current. The modulation index can be selected as $0 \leq m_c \leq 1$, and the maximum current amplitude which can be constructed with this modulation method is $i_{pn,ave}$. The averaged output current and the DC-link voltage of this current source converter is as follows:

$$\vec{I}_{i,ave} = Di_k\vec{I}_k + Di_{k+1}\vec{I}_{k+1} + Di_0\vec{I}_0 = \vec{I}_{i,ref}, \tag{7}$$

$$v_{pn,ave} = \frac{3}{2i_{pn}}\{Di_k\vec{I}_k.\vec{V}_i + Di_{k+1}\vec{I}_{k+1}.\vec{V}_i\}$$

$$= \frac{3}{2}m_cV_i\cos\varphi_i, \tag{8}$$

where, V_i and φ_i are the instantaneous input phase-neutral voltage amplitude and phase angle with respect to the input current.

2.1.3. SVM of the indirect matrix converter

SVM of an indirect matrix converter is a combination of voltage source and current source converters modulations. To construct the desired output voltage vector $\vec{V}_{o,ref}$ in the sector ⓙand desired input current vector $\vec{I}_{i,ref}$ in the sector ⓚ vectors $\vec{V}_j$ and $\vec{V}_{j+1}$ in the voltage source converter, and vectors $\vec{I}_k$ and $\vec{I}_{k+1}$ in the current source converter are used. For this purpose, as presented in Figure 5, D_{jk} portion of the switching period vectors $\vec{V}_j$ and $\vec{I}_k$, $D_{j(k+1)}$ portion of the switching period vectors $\vec{V}_j$ and $\vec{I}_{k+1}$, $D_{(j+1)k}$ portion of the switching period vectors $\vec{V}_{j+1}$ and $\vec{I}_k$, and $D_{(j+1)(k+1)}$ portion of the switching period vectors

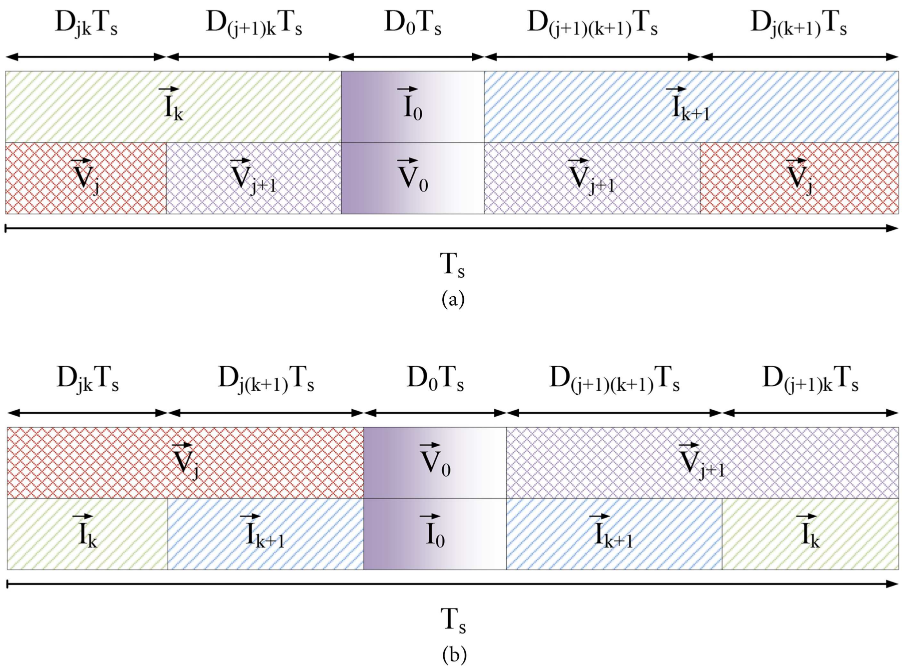

Figure 5. The indirect matrix converter space vector modulation patterns.

$\vec{V}_{j+1}$ and $\vec{I}_{k+1}$ are applied. And for the last remaining part of the switching period (i.e., D_0), vectors $\vec{V}_0$ and $\vec{I}_0$ are applied. Where D_{jk}, $D_{j(k+1)}$, $D_{(j+1)k}$, $D_{(j+1)(k+1)}$ and D_0 are calculated form Eqs. (1) and (5) as presented in Eq. (9). Similar to Figure 5(a) and (b), order of applying input, output and zero vectors can be changed arbitrary to reduce the switching frequency and loss or the output voltages and input currents distortion and THD.

$$\begin{cases} D_{jk} = Dv_j Di_k = m_t \sin\left(\frac{\pi}{3} - \theta_o\right) \sin\left(\frac{\pi}{3} - \theta_i\right) \\ D_{j(k+1)} = Dv_j Di_{k+1} = m_t \sin\left(\frac{\pi}{3} - \theta_o\right) \sin\left(\theta_i\right) \\ D_{(j+1)k} = Dv_{j+1} Di_k = m_t \sin\left(\theta_o\right) \sin\left(\frac{\pi}{3} - \theta_i\right) \\ D_{(j+1)(k+1)} = Dv_{j+1} Di_{k+1} = m_t \sin\left(\theta_o\right) \sin\left(\theta_i\right) \\ D_0 = 1 - D_{jk} - D_{j(k+1)} - D_{(j+1)k} - D_{(j+1)(k+1)} \end{cases} \tag{9}$$

where $m_t = m_c m_v$ is the total matrix converter modulation index which can be selected as $0 \leq m_t \leq 1$.

2.2. Voltage and current gains

With the indirect modulation strategy presented in Figure 5, for the Di_k portion of the time duration applying $\vec{V}_j$ in the output converter, $\vec{I}_k$ is applied in the input converter, and for the remaining Di_{k+1} part of this time $\vec{I}_{k+1}$ is applied in the input converter. Also, for the Di_k portion of the time duration applying $\vec{V}_{j+1}$ in the output converter, $\vec{I}_k$ is applied in the input converter, and for the remaining Di_{k+1} part of this time $\vec{I}_{k+1}$ is applied in the input converter. Therefore, the averaged DC-link voltage during applying $\vec{V}_j$, $\vec{V}_{j+1}$ and also the whole of the switching period is the same as Eq. (8), and with respect to Eq. (2), the averaged output phase-neutral voltage vector which can be obtained by the indirect modulation strategy is:

$$V_{o,ave} = \frac{\sqrt{3}}{2} m_t V_i \cos\varphi_i \approx 0.866 m_t V_i \cos\varphi_i. \tag{10}$$

It can be seen that the maximum output phase-neutral voltage which can be constructed with the indirect matrix converter depends on the input power factor of the converter. When the input power factor is one the maximum output phase-neutral voltage is 0.866 of the input phase-neutral voltage.

Similarly, as presented in Figure 5, for the Dv_j portion of the time duration applying $\vec{I}_k$ in the input converter, $\vec{V}_j$ is applied in the output converter, and for the remaining Dv_{j+1} part of this time $\vec{V}_{j+1}$ is applied in the output converter. Also, for the Dv_j portion of the time duration applying $\vec{I}_{k+1}$ in the input converter, $\vec{V}_j$ is applied in the output converter, and for the remaining Dv_{j+1} part of this time $\vec{V}_{j+1}$ is applied in the output converter. Therefore, the averaged DC-link current during applying $\vec{I}_k$, $\vec{I}_{k+1}$ and also the whole of the switching period is the same as Eq. (4), and with respect to Eq. (6), the averaged input current vector which can be obtained by the indirect modulation strategy is:

$$I_{i,ave} = \frac{\sqrt{3}}{2} m_t I_o \cos\varphi_o \approx 0.866 m_t I_o \cos\varphi_o. \tag{11}$$

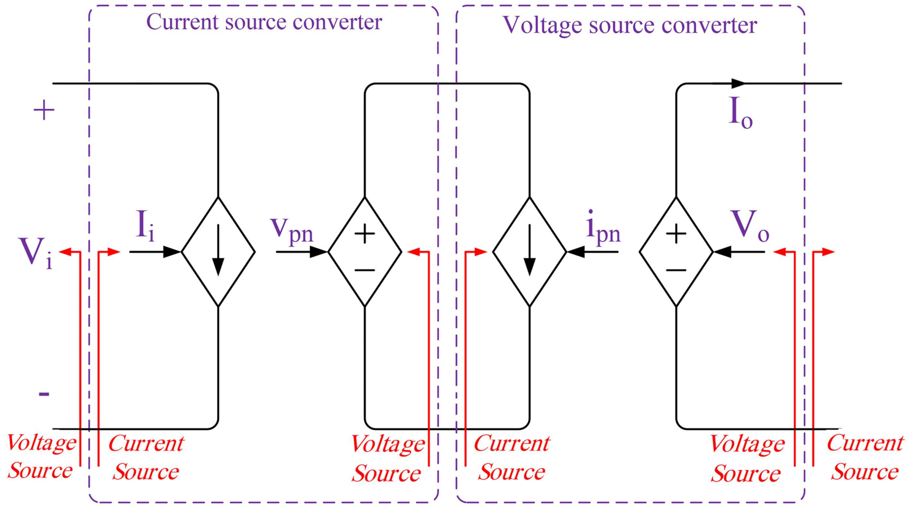

Figure 6. The two-port indirect matrix converter single-phase equivalent circuit.

3. Generalized multi-port indirect matrix converter

The indirect matrix converter is a two-port HFAC converter. However, in a hybrid system a multi-port converter is required to connect two or more AC or DC power resources to an AC or DC grid or load. As presented in Figure 1, conventional back-to-back converters can easily be extended to a multi-port converter by connecting multiple voltage source converter through their common DC link. However, except for a few cases [14-22], most of the matrix and HFAC converters proposed in the literature are two-port converters which can be used to connect a single DG or storage to an AC or DC grid. In this section, a generalized structure of a multi-port indirect matrix converter is proposed which can be used to connect several AC or DC resources to an AC or DC grid or load in a hybrid system.

The single-phase equivalent circuit of a two-port indirect matrix converter is presented in Figure 6. As presented in Figure 2, the input filter of the current source converter is a capacitive filter which is a voltage source element. Therefore, the output port of this converter is also a controllable voltage source with the value presented in Eq. (8). Since two voltage sources with different voltages cannot be paralleled, the output port of this converter must be connected to a current source. In a similar manner, the output filer of the voltage source converter is an inductive filter which is a current source component. Therefore, the input port of this converter is also a controllable current source with the value presented in Eq. (4). Since two current sources with different currents cannot be serried, the input port of this converter must be connected to a voltage source.

Since two or more current sources with different currents can be paralleled, or two or more voltage sources with different voltages can be serried, to extend an indirect matrix (or HFAC) converter to a multi-port converter several voltage source converters can be paralleled in the output stage or several current source converters can be serried in the input stage of an indirect matrix converter. The single-phase equivalent circuit of these multi-port converters are presented in Figure 7 for three-port samples.

Therefore, as presented in Figure 7(a), in a single-input multi-output matrix converter two or more voltage source converters are connected in parallel in the output stage, and as presented in Figure 7(b), in a multi-input single-output matrix converter two or more current source converters are connected in series in the input stage. Where, the voltage and current source converters can be a three-phase, single-phase or a DC converter of Figures 8 and 9 respectively.

3.1. Modulation method

To control a multi-port indirect matrix converter the same as a two-port indirect matrix converter indirect SVM method is proposed in which, the voltage and current source converters are controlled with the conventional SVM method for the three-phase converters or PWM method for single-phase and DC converters. Then, switching states of these converters are combined such that the desired averaged output voltage and input current achieved. This process is described for a single-input multi-output matrix converter and multi-input single-output matrix converters in the two following separate subsections.

3.1.1. Single-input multi-output matrix converter modulation method

To simplify the single-input multi-output matrix converter control and modulation, modulation index of

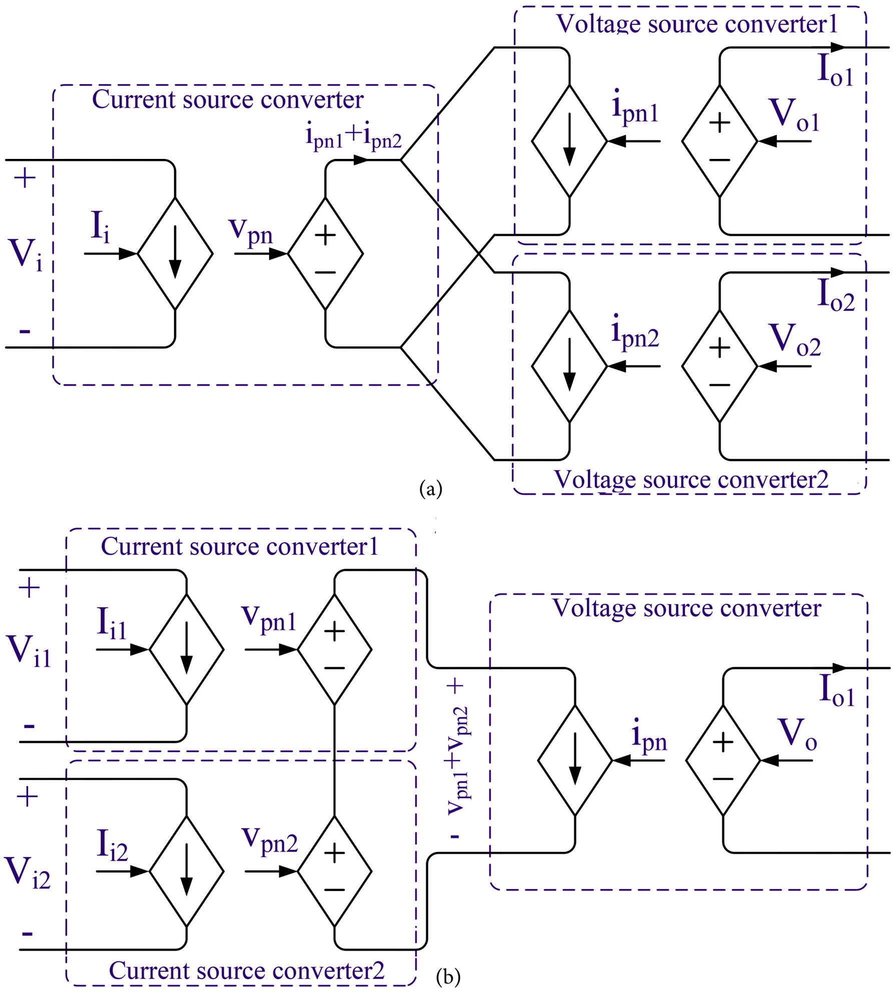

Figure 7. Three-port indirect matrix converters equivalent circuit (a) Single-input multi-output indirect matrix converter equivalent circuit; (b) Multi-input single-output indirect matrix converter equivalent circuit.

the input current source converter (i.e., m_c) is selected as one and the output voltage source converter modulation indexes (i.e., $m_{v1}, m_{v2}, ..., m_{vn}$) are changed to control the outputs voltage and input current of the multi-port matrix converter as follows:

$$m_c = \frac{I_{i,ref}}{i_{pn,ave}} = 1,$$

$$v_{pn,ave} = \frac{3}{2} m_c V_i \cos\varphi_i = \frac{3}{2} V_i \cos\varphi_i,$$

$$i_{pn,ave} = \sum_{l=1}^{n} \frac{\sqrt{3}}{2} m_{vl} I_{ol} \cos\varphi_{ol},$$

$$m_{vl} = \sqrt{3} \frac{V_{ol,ref}}{v_{pn,ave}}, \quad l = 1, ..., n. \tag{12}$$

For the DC outputs, the converters duty cycles are calculated in a similar manner to achieve desirable output voltages. It can be seen from Eq. (12) that the same as an indirect matrix converter, the input and outputs power factor limit the multi-output converter voltage and current gains. After calculating modulation indexes and duty cycles, switching times of each vector of the input and output converters are calculated using Eqs. (1) and (5), and the switching states and times of the multi-port converter is calculated by combining the input and each output switching states and times with respect to Eq. (9) and Figure 10(a).

With respect to Figure 7(a), in the single-input multi-output matrix converter, the input current source converter is common between the output voltage source converters. Therefore, as depicted in Figure 10(a), for the input converter, at the first Di_k part of the switching period $\vec{I}_k$, the next Di_0 part of the switching period $\vec{I}_0$, and at the last Di_{k+1} part of the switching period $\vec{I}_{k+1}$ of the input converter are applied. Since each output converter works independent of the other ones, its switching diagram is completely similar to the two-port matrix converter presented in

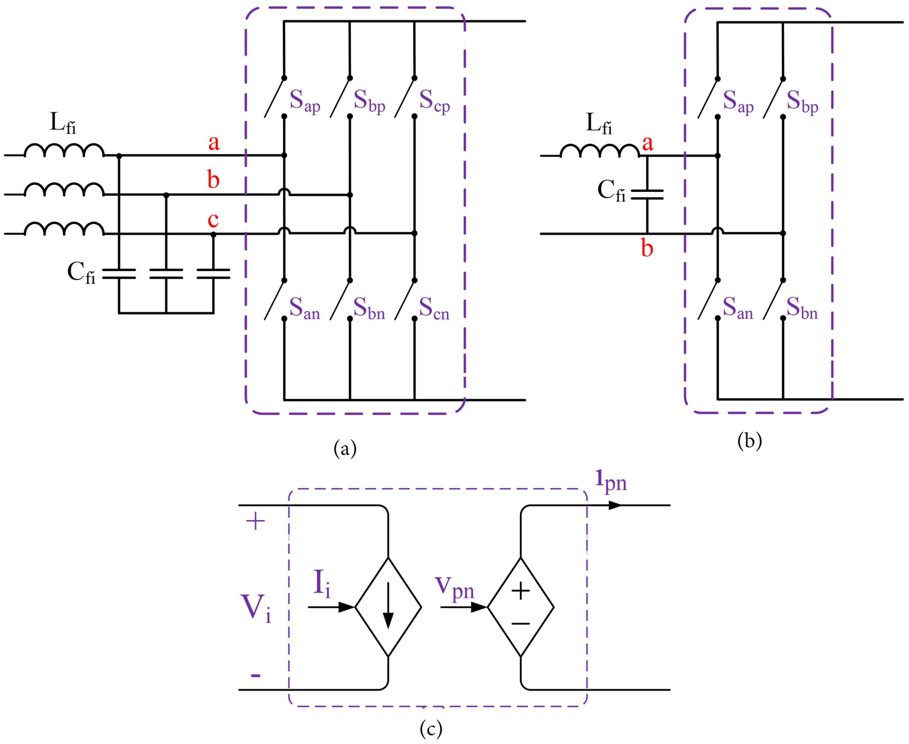

Figure 8. (a) Three-phase current source converter; (b) Single-phase and DC current source converters; and (c) Their single-phase equivalent circuit.

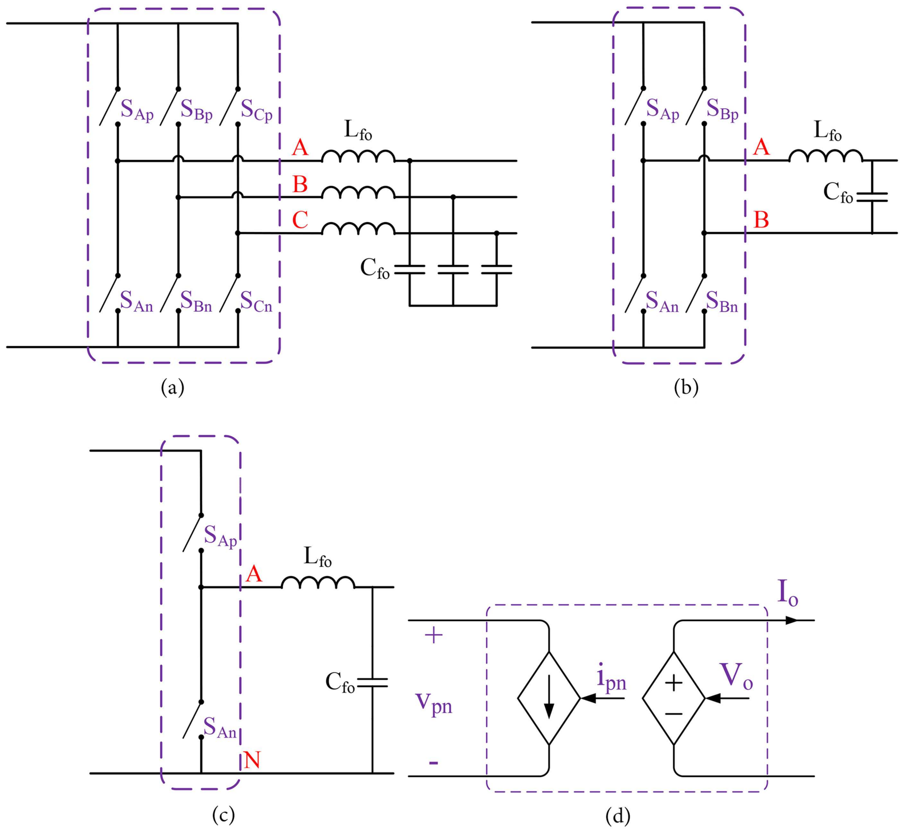

Figure 9. (a) Three-phase voltage source converter; (b) Full-bridge single-phase and DC voltage source converters; (c) Half-bridge DC voltage source converter; and (d) Their single-phase equivalent circuit.

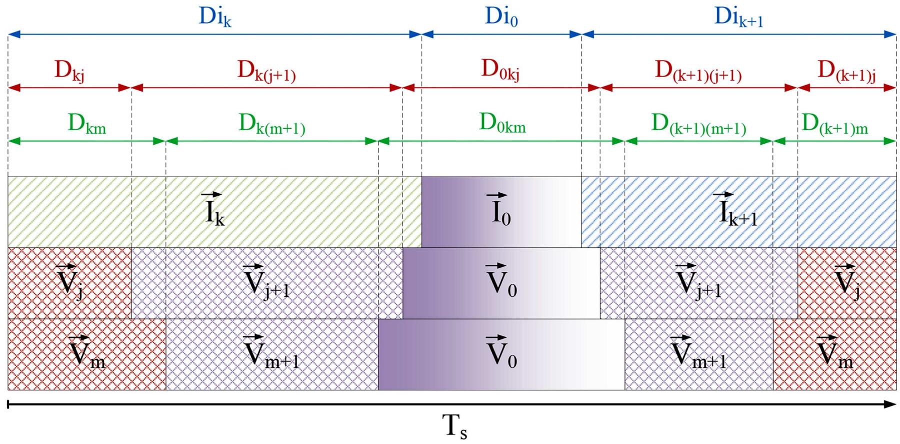

(a)

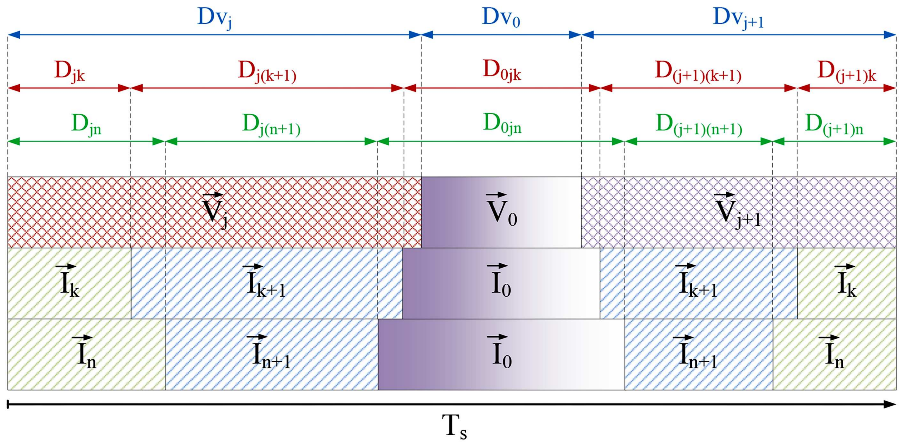

(b)

Figure 10. Switching states and timing diagram of the multi-port indirect matrix converter (a) Single-input multi-output converter and (b) multi-input single-output converter.

Figure 5(a). Therefore, for the typical converter which is in sector j, at the first D_{kj} part of the switching period $\vec{V}_j$, the next $D_{k(j+1)}$ part of the switching period $\vec{V}_{j+1}$, the next D_{0kj} part of the switching period $\vec{V}_0$, the next $D_{(k+1)(j+1)}$ part of the switching period $\vec{V}_{j+1}$, and at the last $D_{(k+1)j}$ part of the switching period $\vec{V}_j$ of the input converter are applied. With this modulation method, each output port operates with the input port similar to a two-port matrix converter.

3.1.2. Multi-input single-output matrix converter modulation method

In a similar manner, to control the multi-input single-output matrix converter simply, modulation index of the output voltage source converter (i.e., m_v) is selected as one and the input current source converter modulation indexes (i.e., $m_{c1}, m_{c2}, ..., m_{cn}$) are changed to control the output voltage and inputs current of the matrix converter as follows:

$$m_v = \sqrt{3}\frac{V_{o,ref}}{v_{pn,ave}} = 1,$$

$$i_{pn,ave} = \frac{\sqrt{3}}{2}m_v I_o \cos\varphi_o = \frac{\sqrt{3}}{2}I_o \cos\varphi_o,$$

$$v_{pn,ave} = \sum_{l=1}^{n}\frac{3}{2}m_{cl}V_{il}\cos\varphi_{il},$$

$$m_{cl} = \frac{I_{il,ref}}{i_{pn,ave}}, \quad l = 1, ..., n. \tag{13}$$

For the DC inputs, the converters duty cycles are calculated in a similar manner to achieve desirable input. It can be seen from Eq. (13) that the same as an indirect matrix converter, the inputs and output power factor limit the multi-input converter voltage and current gains. After calculating modulation indexes and duty cycles, switching times of each vector of the input and output converters are calculated using Eqs.

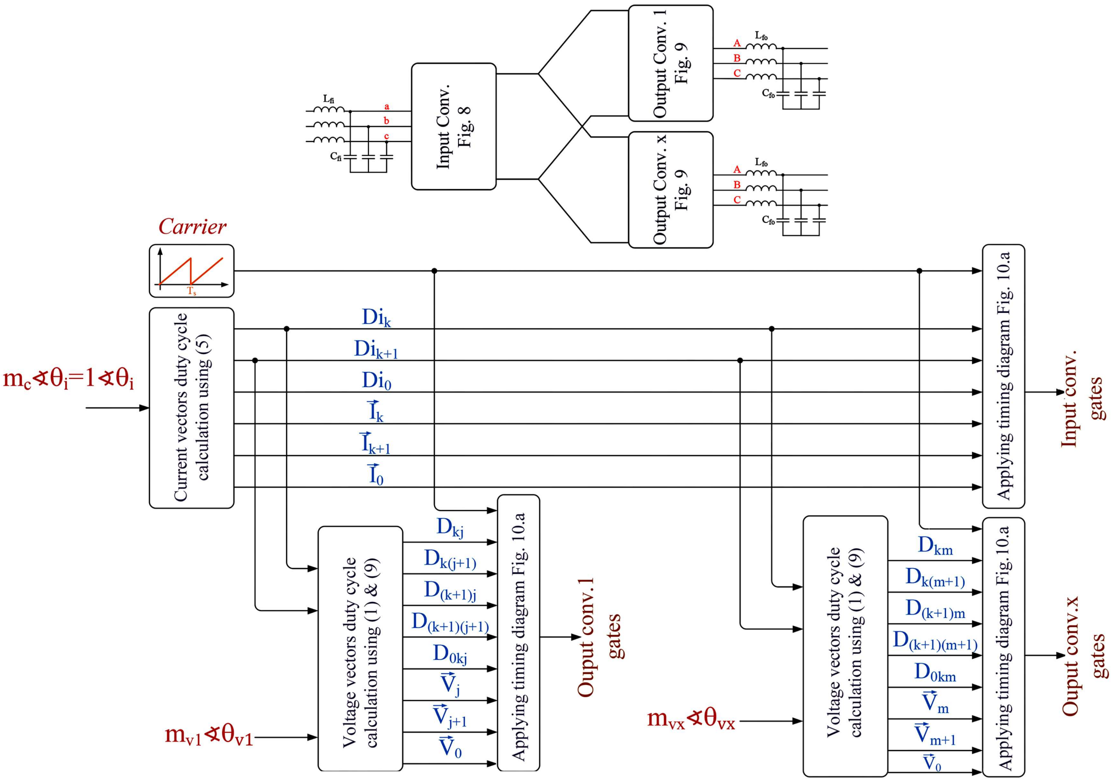

Figure 11. The general scheme of the simulated single-input multi-output converters and their control structure.

(1) and (5), and the switching states and times of the multi-port converter is calculated by combining the input and each output switching states and times with respect to Eq. (9) and Figure 10(b).

With respect to Figure 7(b), in the multi-input single-output matrix converter, the output voltage source converter is common between the input current source converters. Therefore, as depicted in Figure 10(b), for the output converter, at the first Dv_j part of the switching period $\vec{V}_j$, the next Dv_0 part of the switching period $\vec{V}_0$, and at the last Dv_{j+1} part of the switching period $\vec{V}_{j+1}$ of the output converter are applied. Since each input converter works independent of the other ones, its switching diagram is completely similar to the two-port matrix converter presented in Figure 5(b). Therefore, for the typical converter which is in sector k, at the first D_{jk} part of the switching period $\vec{I}_k$, the next $D_{j(k+1)}$ part of the switching period $\vec{I}_{k+1}$, the next D_{0jk} part of the switching period $\vec{I}_0$, the next $D_{(j+1)(k+1)}$ part of the switching period $\vec{I}_{k+1}$, and at the last $D_{(j+1)k}$ part of the switching period $\vec{I}_k$ of the input converter are applied. With this modulation method, each input port operates with the output port similar to a two-port matrix converter.

4. Simulation results

In this section, the proposed generalized structure is evaluated through simulation in the MATLAB/SIMULINK software environment. For this purpose, a single-input multi-output and a multi-input single-output indirect matrix converter are considered in the two following subsections.

4.1. Single-input multi-output indirect matrix converter

A single-input multi-output indirect matrix converter can be used to connect different three-phase, single-phase, or DC systems to each other. In these simulations, three single-input multi-output converters are simulated in three cases. The first one connects a three-phase input system to the two different three-phase output systems, the second one is used to connect a three-phase input system to a three-phase and a DC output systems, and finally, the third one is used to connect a three-phase input system to the three different three-phase output systems. The general scheme of the simulated systems and their control structure is presented in Figure 11. Circuit diagram of the three-phase input current source converter is presented in Figure 8(a), and the circuit diagram of the output three-phase and DC voltage source converters are presented in Figure 9(a) and (b) respectively. The parameters of the input and output stages are presented in Table 3.

4.1.1. Single-input double-output AC→AC-AC converter

Table 3. Simulation parameters of the single-input multi-output indirect matrix converters.

AC input	V_i	400 V
	f_i	50 Hz
	$\cos\phi_i$	1
	L_{fi}	500 μH
	C_{fi}	20 μF
AC output 1	V_o	200 V
	f_o	60 Hz
	Z_{Load}	10 $\Omega\angle 36.78^o$
	L_{fo}	5 mH
	C_{fo}	1 μF
AC output 2 (case 1 & case 3)	V_o	100 V
	f_o	75 Hz
	R_{Load}	5 Ω
	L_{fo}	5 mH
	C_{fo}	1 μF
DC output 2 (case 2)	V_o	100 V
	R_{Load}	10 Ω
	L_{fo}	10 mH
	C_{fo}	5 μF
AC output 3 (case 3)	V_o	75 V
	f_o	50 Hz
	R_{Load}	5 $\Omega\angle 36.78^o$
	L_{fo}	5 mH
	C_{fo}	1 μF
Switching frequency	f_s	20 kHz

In this case, to examine the converter performance, at time 0.025 s the input power factor is changed from 1 to 0.8, and at time 0.05 s the AC output 2 voltage is increased 50% and simulation results for this converter is presented in Figure 12.

4.1.2. Single-input double-output AC→AC-DC converter
Similar to the previous case, in this case, at time 0.025 s the input power factor is changed from 1 to 0.8, and at time 0.05 s the DC output 2 voltage is increased 50% and simulation results of this converter is also presented in Figure 13.

4.1.3. Single-input triple-output AC→AC-AC-AC converter
Similar to the two previous cases, at time 0.025 s the input power factor is changed from 1 to 0.8, and at time 0.05 s the AC output 2 voltage is increased 50% and simulation results for this converter is presented in Figure 14.

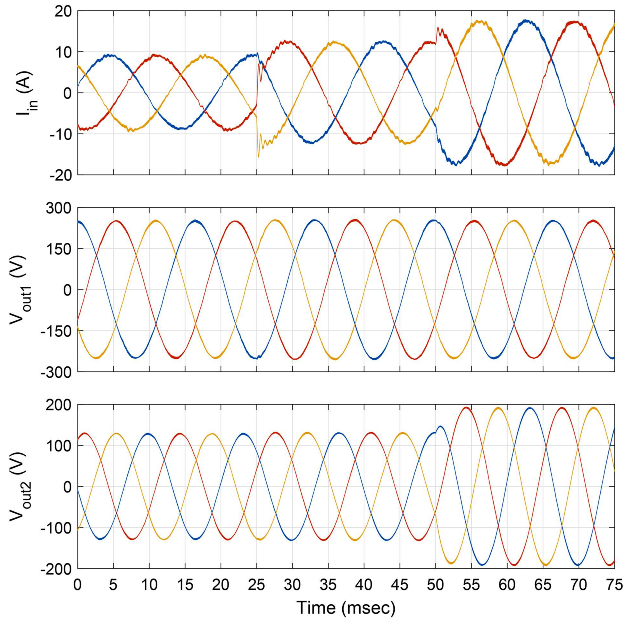

Figure 12. Simulation results of single-input double-output AC→AC-AC converter. I_{in}: AC input current; V_{out1}: AC output 1 line-to-line voltage; V_{out2}: AC output 2 line-to-line voltage.

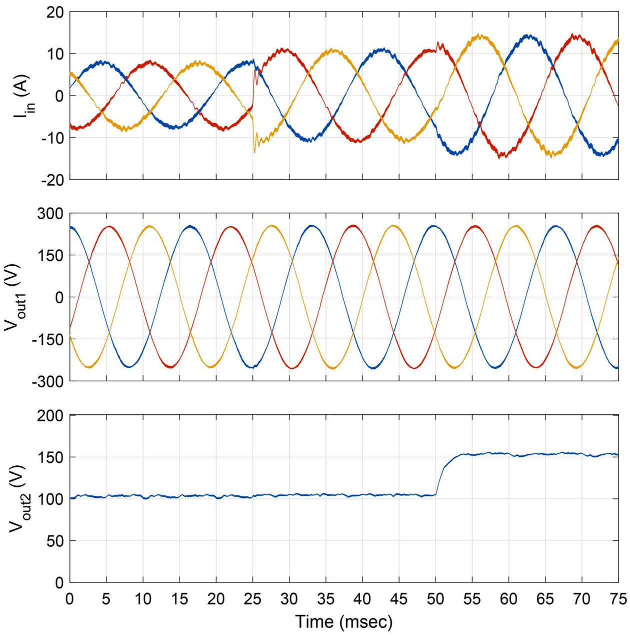

Figure 13. Simulation results of single-input double-output AC→AC-DC converter. I_{in}: AC input current; V_{out1}: AC output line-to-line voltage; V_{out2}: DC output voltage.

4.2. Multi-input single-output indirect matrix converter

Similarly, a multi-input single-output indirect matrix converter can be used to connect different three-phase, single-phase, or DC systems to each other. In these simulations, three multi-input single-output converters are simulated in three cases which, the first one

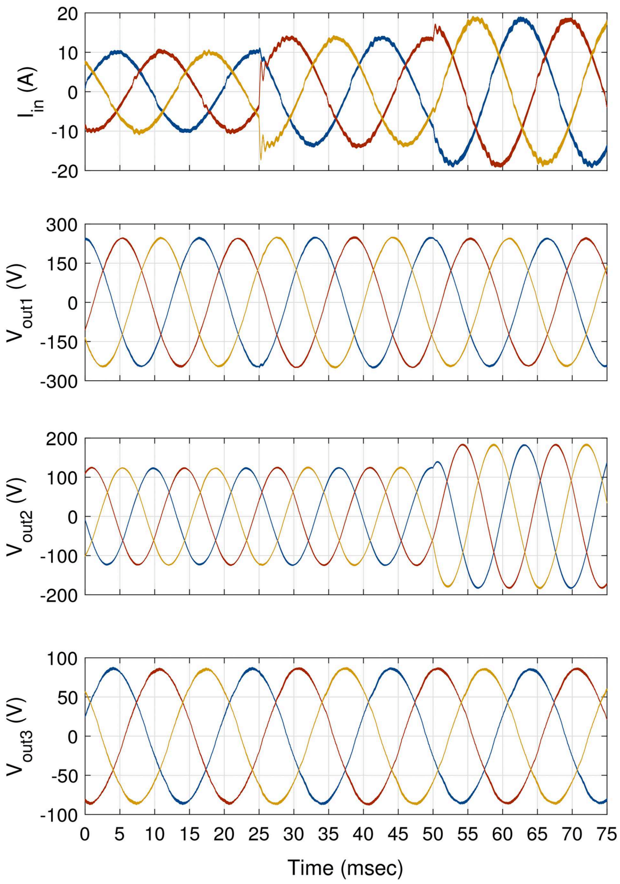

Figure 14. Simulation results of single-input triple-output AC→AC-AC-AC converter. I_{in}: AC input current; V_{out1}: AC output 1 line-to-line voltage; V_{out2}: AC output 2 line-to-line voltage; V_{out3}: AC output 3 line-to-line voltage.

connects two different three-phase input systems to a three-phase output system, the second one is used to connect a three-phase and a DC input systems to a three-phase output system, and finally, the third one is used to connect three different three-phase input systems to a three-phase output system. The general scheme of the simulated systems and their control structure is presented in Figure 15. Circuit diagram of the three-phase and DC input current source converters are presented in Figure 8(a) and (b) respectively, and the circuit diagram of the output three-phase voltage source converters is presented in Figure 9(a). The parameters of the input and output stages are presented in Table 4.

4.2.1. Double-input single-output AC-AC→AC converter

In this case to examine the converter performance, to decrease the AC input 1 power at time 0.025 s its power factor is changed from 1 to 0.8, and at time 0.05 s the AC output voltage is increased 50% and simulation results for this converter is presented in Figure 16.

Table 4. Simulation parameters of the multi-input single-output indirect matrix converters.

AC input 1	V_i	400 V
	f_i	50 Hz
	$\cos \phi_i$	1
	L_{fi}	500 μH
	C_{fi}	20 μF
AC input 2 (case 1 & case 3)	V_i	150 V
	f_i	75 Hz
	$\cos \phi_i$	0.85
	L_{fi}	500 μH
	C_{fi}	20 μF
DC input 2 (case 2)	V_i	100 V
	L_{fi}	500 μH
	C_{fi}	20 μF
AC input 3 (case 3)	V_i	75 V
	f_i	50 Hz
	$\cos \phi_i$	0.75
	L_{fi}	500 μH
	C_{fi}	20 μF
AC output	V_o	200 V
	f_o	60 Hz
	R_{Load}	10 Ω
	L_{fo}	5 mH
	C_{fo}	1 μF
Switching frequency	f_s	20 kHz

4.2.2. Double-input single-output AC-DC→AC converter

Similar to the previous case, in this case to decrease the DC input 2 power at time 0.025 s its modulation index is changed from 1 to 0.8, and at time 0.05 s the AC output voltage is increased 50% and simulation results of this converter is also presented in Figure 17.

4.2.3. Triple-input single-output AC-AC-AC→AC converter

In this case, similar to the two previous cases, to decrease the AC input 1 power at time 0.025 s its power factor is changed from 1 to 0.8, and at time 0.05 s the AC output voltage is increased 50% and simulation results for this converter is presented in Figure 18.

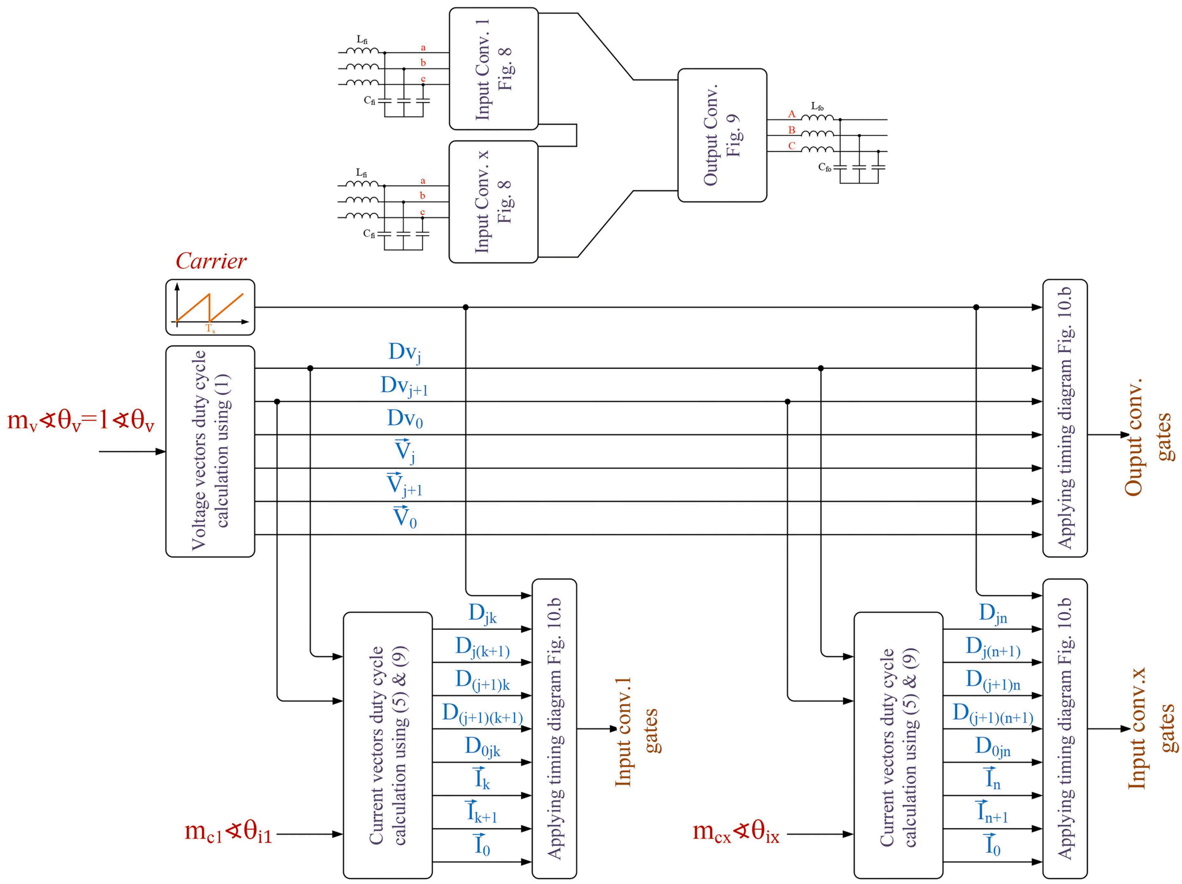

Figure 15. The general scheme of the simulated multi-input single-output converters and their control structure.

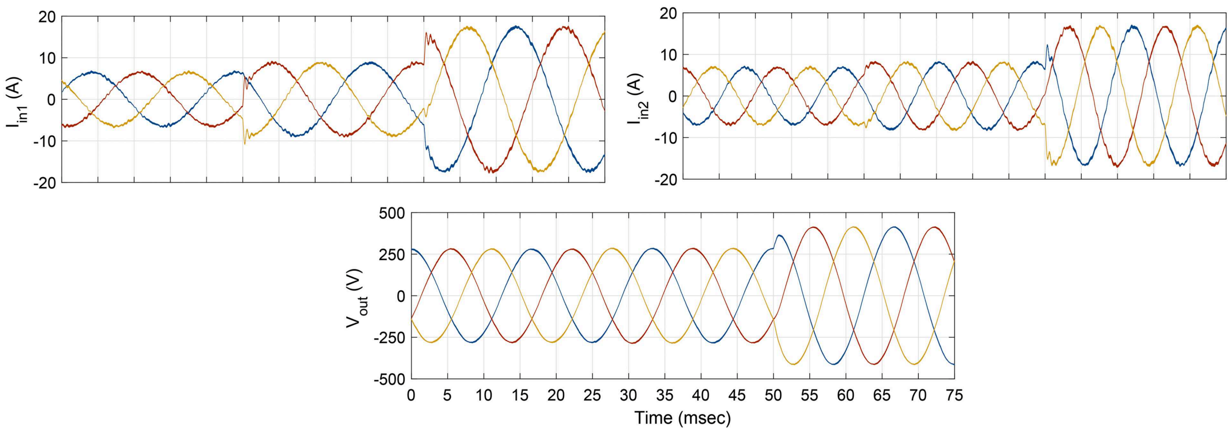

Figure 16. Simulation results of double-input single-output AC-AC→AC converter. I_{in1}: AC input 1 current; I_{in2}: AC input 2 current; V_{out}: AC output line-to-line voltage.

5. Conclusions

To connect multiple Distributed Generators (DGs) and storages to an AC or DC grid or load a multi-port converter is required. Conventional back-to-back converters can easily be extended to a multi-port converter by connecting several voltage source converters through their common DC link. Bulky DC link capacitor simplifies converter control and extension, but increases the system volume and reduces its life time. Common high frequency AC-link converters such as indirect matrix converters are two-port converters. In this paper a general structure for a multi-port indirect matrix converter is proposed which can be used to connect several DC or AC resources to an AC or DC grid or load. The proposed structure can be used to

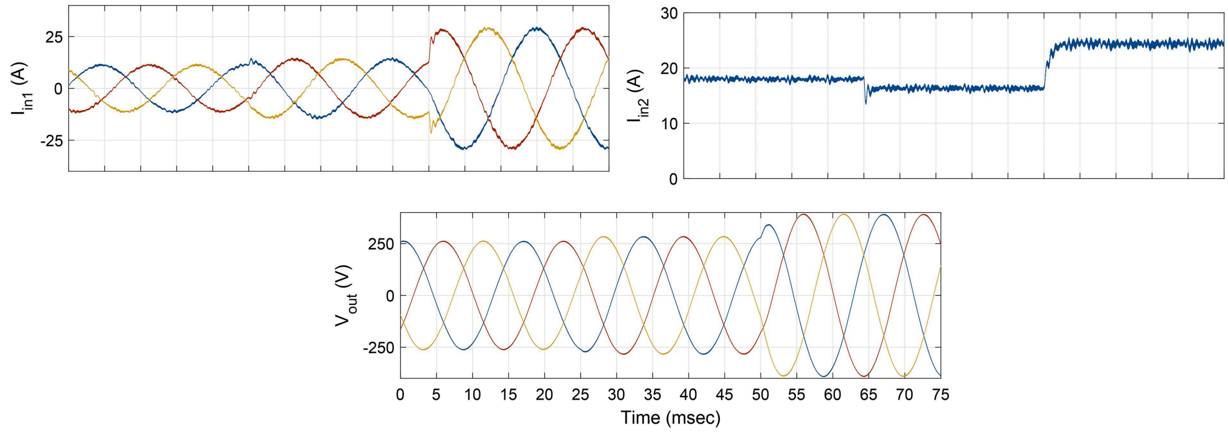

Figure 17. Simulation results of double-input single-output AC-DC→AC converter. I_{in1}: AC input current; I_{in2}: DC input current; V_{out}: AC output line-to-line voltage.

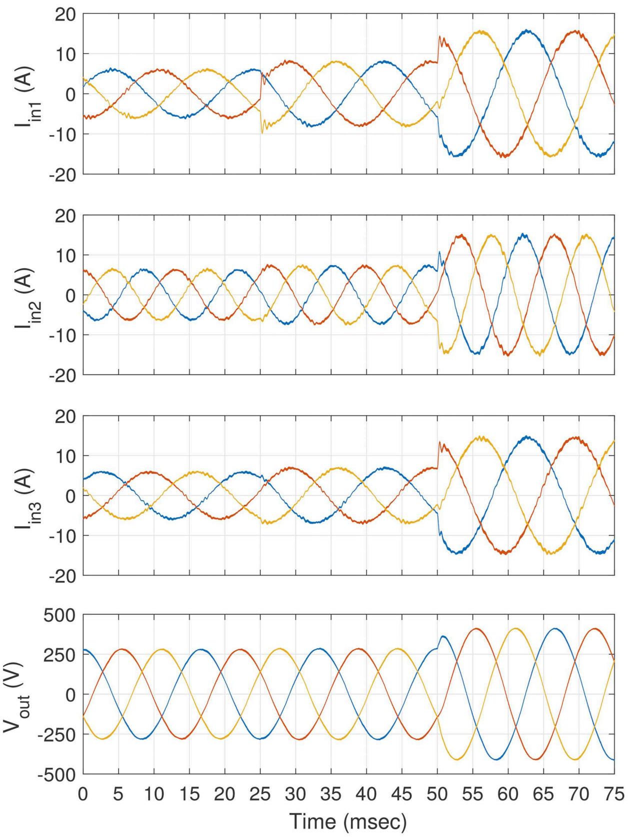

Figure 18. Simulation results of triple-input single-output AC-AC-AC→AC converter. I_{in1}: AC input 1 current; I_{in2}: AC input 2 current; I_{in3}: AC input 3 current; V_{out}: AC output line-to-line voltage.

extend every HFAC converter to a multi-port converter. The modulation method and voltage and current gain of the proposed converter are also presented.

References

1. Khosrogorji, S., Ahmadian, M., Torkaman, H., et al. "Multi-input dc/dc converters in connection with distributed generation units-a review", *Renewable and Sustainable Energy Reviews*, **66**, pp. 360–379 (2016). https://doi.org/10.1016/j.rser.2016.07.023
2. Bairabathina, S. and Balamurugan, S. "Review on non-isolated multi-input step-up converters for grid-independent hybrid electric vehicles", *International Journal of Hydrogen Energy*, **45**(41), pp. 21687–21713 (2020). https://doi.org/10.1016/j.ijhydene.2020.05.277
3. Zhang, T., Jiang, J., and Chen, D. "An efficient and low-cost dmppt approach for photovoltaic submodule based on multi-port dc converter", *Renewable Energy*, **178**, pp. 1144–1155 (2021). https://doi.org/10.1016/j.renene.2021.06.134
4. Affam, A., Buswig, Y.M., Othman, A.-K.B.H., et al. "A review of multiple input dc-dc converter topologies linked with hybrid electric vehicles and renewable energy systems", *Renewable and Sustainable Energy Reviews*, **135**, p. 110186 (2021). https://doi.org/10.1016/j.rser.2020.110186
5. Bizhani, H., Noroozian, R., Muyeen, S., et al. "Grid integration of multiple wind turbines using a multi-port converter–a novel simultaneous space vector modulation", *Renewable and Sustainable Energy Reviews*, **157**, 111940 (2022). https://doi.org/10.1016/j.rser.2021.111940
6. Blaabjerg, F., Teodorescu, R., Liserre, M., et al. "Overview of control and grid synchronization for distributed power generation systems", *IEEE Transactions on Industrial Electronics*, **53**(5), pp. 1398–1409 (2006). https://doi.org/10.1109/TIE.2006.881997
7. Wang, H., Liserre, M., and Blaabjerg, F. "Toward reliable power electronics: Challenges, design tools, and opportunities", *IEEE Industrial Electronics Magazine*, **7**(2), pp. 17–26 (2013). https://doi.org/10.1109/MIE.2013.2252958
8. Al-Shetwi, A.Q., Sujod, M.Z., Blaabjerg, F., et al. "Fault ride-through control of grid-connected photovoltaic power plants: A

review", *Solar Energy*, **180**, pp. 340–350 (2019). https://doi.org/10.1016/j.solener.2019.01.032

9. Taul, M.G., Wang, X., Davari, P., et al. "Robust fault ride through of converter-based generation during severe faults with phase jumps", *IEEE Transactions on Industry Applications*, **56**(1), pp. 570–583 (2019). https://doi.org/10.1109/TIA.2019.2944175
10. Zeb, K., Islam, S.U., Khan, I., et al. "Faults and fault ride through strategies for grid-connected photovoltaic system: A comprehensive review", *Renewable and Sustainable Energy Reviews*, **158**, 112125 (2022). https://doi.org/10.1016/j.rser.2022.112125
11. Yushan, L., Jie, H., Baoming, G., et al. "A simple space vector modulation of high-frequency ac linked three-phase-to-single-phase/dc converter", *IEEE Access*, **8**, pp. 278–289 (2020). https://doi.org/10.1109/ACCESS.2020.2978886
12. Friedli, T., Kolar, J.W., Rodriguez, J., et al. "Comparative evaluation of three-phase ac-ac matrix converter and voltage dc-link back-to-back converter systems", *IEEE Transactions on Industrial Electronics*, **59**(12), pp. 4487–4510 (2012). https://doi.org/10.1109/TIE.2011.2179278
13. Empringham, L., Kolar, J.W., Rodriguez, J., et al. "Technological issues and industrial application of matrix converters: A review", *IEEE Transactions on Industrial Electronics*, **60**(10), pp. 4260–4271 (2013). https://doi.org/10.1109/TIE.2012.2216231
14. Klumpner, C. and Blaabjerg, F. "Modulation method for a multiple drive system based on a two-stage direct power conversion topology with reduced input current ripple", *IEEE Transactions on Power Electronics*, **20**(4), pp. 922–929 (2005). https://doi.org/10.1109/TPEL.2005.850965
15. Kato, K. and Itoh, J.-i. "Control method for a three-port interface converter using an indirect matrix converter with an active snubber circuit", *Power Electronics and Motion Control Conference*, 2008. EPE-PEMC 2008. 13th, pp. 581–588 (2008). https://doi.org/10.1109/EPEPEMC.2008.4635328
16. Kato, K. and Itoh, J.-i. "An investigation of high efficiency operation conditions for a three-port energy source system using an indirect matrix converter", *Energy Conversion Congress and Exposition (ECCE)*, 2011 IEEE, pp. 230–237 (2011). https://doi.org/10.1109/ECCE.2011.6063774
17. Liu, X., Wang, P., Loh, P.C., et al. "A compact three-phase single-input/dual-output matrix converter", *IEEE Transactions on Industrial Electronics*, **59**(1), pp. 6–16 (2011). https://doi.org/10.1109/TIE.2011.2146216
18. Milan, G., Dehghan, S., Biabani, M., et al. "Single-input-dual-output matrix converters and space vector modulation", *20th Iranian Conference on Electrical Engineering (ICEE2012)*, pp. 569–574 (2012). https://doi.org/10.1109/IranianCEE.2012.6292421
19. Liu, X., Wang, P., Loh, P.C., et al. "A three-phase dual-input matrix converter for grid integration of two ac type energy resources", *IEEE Transactions on Industrial Electronics*, **60**(1), pp. 20–30 (2012). https://doi.org/10.1109/TIE.2012.2183838
20. Bak, Y., Lee, E., and Lee, K.-B. "An indirect matrix converter for dual output ac-drive system with reduced number of power transistors", *2014 IEEE Conference on Energy Conversion (CENCON)*, pp. 360–364 (2014). https://doi.org/10.1109/CENCON.2014.6967530
21. Wang, H., Su, M., Sun, Y., et al. "Active third-harmonic injection indirect matrix converter with dual three-phase outputs", *IET Power Electronics*, **9**(4), pp. 657–668 (2016). https://doi.org/10.1049/iet-pel.2014.0703
22. Sadooghi, R., Niknam, T., Sheikh, M., et al. "An effective non-square matrix converter based approach for active power control of multiple dgs in microgrids: Experimental implementation", *IEEE Transactions on Energy Conversion*, **37**(2), pp. 755–765 (2021). https://doi.org/10.1109/TEC.2021.3116310
23. Alammari, R., Aleem, Z., Iqbal, A., et al. "Matrix converters for electric power conversion: Review of topologies and basic control techniques", *International Transactions on Electrical Energy Systems*, **29**(10), e12063 (2019). https://doi.org/10.1002/2050-7038.12063
24. Patel, P.P. and Mulla, M.A. "A single carrier-based pulsewidth modulation technique for three-to-three phase indirect matrix converter", *IEEE Transactions on Power Electronics*, **35**(11), pp. 589–601 (2020). https://doi.org/10.1109/TPEL.2020.2988594
25. Tran, Q.-H., Nguyen, T.D., and Phuong, L.M. "Simplified space-vector modulation strategy for indirect matrix converter with common-mode voltage and harmonic distortion reduction", *IEEE Access*, **8**, pp. 489–498 (2020). https://doi.org/10.1109/ACCESS.2020.3042528
26. Huber, L. and Borojevic, D. "Space vector modulated three-phase to three-phase matrix converter with input power factor correction", *IEEE Transactions on Industry Applications*, **31**(6), pp. 1234–1246 (1995). https://doi.org/10.1109/28.475693

Biography

Hossein Hojabri was born in Kerman, Iran, in 1982. He received the BSc degree in electrical engineering from Isfahan University of Technology, Isfahan, Iran, in 2004, and the MSc and PhD degrees in electrical engineering from Sharif University of Technology, Tehran, Iran, in 2006 and 2013, respectively. He is currently an Associate Professor with the Department of Electrical Engineering, Shahid Bahonar University of Kerman, Kerman, Iran. His research interests include application of power electronics in power systems, microgrids, power quality, and renewable energy systems.